FIELD AND CONSTITUTIVE EQUATIONS FOR A TWO-PHASE MEDIUM FOR ANALYSIS OF THE BEHAVIOR OF IN-SITU SOIL DEPOSITS

Jean H. Prévost[I]

SUMMARY

Field and constitutive equations for the treatment of soil as a two-phase medium in boundary value problems are presented. A number of examples which demonstrate the versatility and accuracy of the proposed formulation are shown.

INTRODUCTION

Soil consists of an assemblage of particles with different sizes and shapes which form a skeleton whose voids are filled with various fluids. In cases in which some flow of the pore fluids takes place, there is an interaction between the skeleton strains and the pore-fluid flow. The solution of these problems therefore requires that soil behavior be analyzed by incorporating the effects of the flow (transient or steady) of the pore-fluids through the voids, and thus requires that a multiphase continuum formulation be available for soils. Such a theory was first developed by Biot [2] for an elastic porous skeleton. However, it is observed experimentally that the stress-strain behavior of the soil skeleton is strongly anelastic. An extension of Biot's theory into the nonlinear anelastic range is therefore necessary in order to analyze the transient response of soil deposits. Such an extension [10] of Biot's formulation is adopted herein. In order to relate the changes in effective stresses carried by the soil skeleton to the skeleton rate of deformations, a general analytical model [9] which describes the nonlinear, anisotropic, elastoplastic, stress and strain dependent, stress-strain-strength properties of the soil skeleton when subjected to complicated three-dimensional, and in particular to cyclic loading paths [7], is used. The model's extreme versatility and accuracy are demonstrated by applying it to represent the behavior of both cohesive and cohesionless soils under both drained and undrained, monotonic and cyclic loading conditions. The use of the proposed formulation for solving boundary value problems is thereafter illustrated.

FIELD EQUATIONS

For a saturated soil consisting of a macroscopically perfect fluid and a piecewise-linear time-independent porous skeleton wherein both the pore-fluid and the solid grains are incompressible, the coupled field equations take the following forms [10],

$$\operatorname{div}[\overset{\nabla}{\underset{\sim}{\sigma}}{}'^{s} + \underset{\sim}{\sigma}'^{s} \operatorname{div} \underset{\sim}{v}^{s}] - \operatorname{div}[(\dot{p}_w + p_w \operatorname{div} \underset{\sim}{v}^{s})\underset{\sim}{1}] + \operatorname{div}[\underset{\sim}{D}:\underset{\sim}{L}^{s}] + \rho_w \operatorname{div} \underset{\sim}{v}^{s}(\underset{\sim}{b}-\underset{\sim}{a}^{w}) + \rho\dot{\underset{\sim}{b}} = \rho^{s}\dot{\underset{\sim}{a}}^{s} + \rho^{w}\dot{\underset{\sim}{a}}^{w} \qquad (1)$$

$$- \operatorname{div}[\frac{n^{w}}{\rho_w} \underset{\sim}{k}^{ws}\cdot(\operatorname{grad} p_w - \rho_w \underset{\sim}{b} + \rho_w \underset{\sim}{a}^{w})] + \operatorname{div} \underset{\sim}{v}^{s} = 0 \qquad (2)$$

in which

[I] Asst. Prof. Civil Eng., Princeton University, Princeton, New Jersey.

$$D_{abcd} = \frac{1}{2}\left[\sigma_{bd}\delta_{ac} - \sigma_{ad}\delta_{bc} - \sigma_{ac}\delta_{bd} - \sigma_{bc}\delta_{ad}\right] \tag{3}$$

is a tensor arising from geometric changes; $\underset{\sim}{\sigma} = \underset{\sim}{\sigma}'^{s} - p_w \underset{\sim}{1}$ is the total stress tensor [33]; and the subscript s and w refer to the solid and fluid phases, respectively. In Eqs. 1 and 2, σ'^{s} = effective Cauchy stress tensor; p_w = pore-fluid pressure; $\underset{\sim}{v}^{\alpha}$ = velocity of α-phase; $\underset{\sim}{a}^{\alpha}$ = acceleration of α-phase; $\underset{\sim}{d}^{\alpha}$ and $\underset{\sim}{w}^{\alpha}$ = symmetric and skew-symmetric parts of the velocity gradient $\underset{\sim}{L}^{\alpha}$, respectively; $\underset{\sim}{k}^{ws}$ = permeability tensor; ρ_{α} = microscopic mass density of α-phase; n^w = porosity; $\rho^s = (1-n^w)\rho_s$; $\rho = \rho^s + n^w\rho_w$; $\underset{\sim}{b}$ = body force density per unit mass; and a superimposed dot indicates the material derivative following the motion of the solid skeleton. In Eq. 1, $\overset{\nabla}{\underset{\sim}{\sigma}}'^{s}$ denotes the Jaumann derivative viz.

$$\overset{\nabla}{\underset{\sim}{\sigma}}'^{s} = \dot{\underset{\sim}{\sigma}}'^{s} + \underset{\sim}{\sigma}'^{s}\cdot\underset{\sim}{w}^{s} - \underset{\sim}{w}^{s}\cdot\underset{\sim}{\sigma}'^{s} \tag{4}$$

CONSTITUTIVE EQUATIONS

The constitutive equations for the solid skeleton are written in one of the following forms [4]:

$$\underset{\sim}{C} : \underset{\sim}{d}^{s} = \begin{cases} \dot{\underset{\sim}{\sigma}}'^{s} & \text{small deformations} \\ \overset{\nabla}{\underset{\sim}{\sigma}}'^{s} + \underset{\sim}{\sigma}'^{s}\,\mathrm{div}\,\underset{\sim}{v}^{s} & \text{finite deformations} \end{cases} \tag{5}$$

C_{abcd} is an (objective) tensor valued function of, possibly, $\underset{\sim}{\sigma}'^{s}$ and the deformation gradients. Many nonlinear material models of interest can be put in the above form (e.g. all nonlinear elastic materials, and many elasto-plastic materials). For soil media [9],

$$\underset{\sim}{C} = \underset{\sim}{E} - \frac{1}{H' + \underset{\sim}{Q}:\underset{\sim}{E}:\underset{\sim}{P}} (\underset{\sim}{E}:\underset{\sim}{P})(\underset{\sim}{Q}:\underset{\sim}{E}) \tag{6}$$

in which H' is the plastic modulus; $\underset{\sim}{P}$ and $\underset{\sim}{Q}$ are dimensionless symmetric second-order tensors, normalized in such a way that $\underset{\sim}{P}:\underset{\sim}{P} = \underset{\sim}{Q}:\underset{\sim}{Q} = 1$ and such that $\underset{\sim}{P}$ gives the direction of plastic deformations and $\underset{\sim}{Q}$ the outer normal to the active yield surface; and $\underset{\sim}{E}$ is the fourth-order tensor of elastic moduli, assumed isotropic for the particular class of material models implemented. The plastic potential is selected such that, in agreement with experimental observations, the plastic deviatoric rate of deformation vector remains normal to the projection of the yield surface onto the deviatoric stress subspace, i.e.,

$$\underset{\sim}{P} - \frac{1}{3}(\mathrm{trace}\ \underset{\sim}{P})\underset{\sim}{1} = \underset{\sim}{Q} - \frac{1}{3}(\mathrm{trace}\ \underset{\sim}{Q})\underset{\sim}{1} = \underset{\sim}{Q}' \tag{7a}$$

$$\text{trace } \underset{\sim}{P} = \text{trace } \underset{\sim}{Q} + A \frac{\text{trace } Q}{|\text{trace } Q|} \{Q':Q'\}^{\frac{1}{2}} \tag{7b}$$

in which A is a material parameter which measures the departure from an associative flow rule. When $A = 0$, $\underset{\sim}{P} = \underset{\sim}{Q}$ and consequently the $\underset{\sim}{C}$ tensor possesses the major symmetry. The yield function is selected of the following form [9]

$$f = \frac{3}{2} (\underset{\sim}{s}^s - \underset{\sim}{\alpha}):(\underset{\sim}{s}^s - \underset{\sim}{\alpha}) + C^2(p'^s - \beta)^2 - k^2 = 0 \tag{8}$$

where $\underset{\sim}{s}^s$ is the deviatoric stress tensor (i.e. $\underset{\sim}{s}^s = \underset{\sim}{\sigma}'^s - p'^s \underset{\sim}{1}$, $p'^s = \frac{1}{3}$ trace σ'^s); α and β are the coordinates of the center of the yield surface in the deviatoric stress space and along the hydrostatic stress axis, respectively; k is the size of the yield surface; and C is a material parameter called the yield surface axis ratio. In order to allow for the adjustment of the plastic hardening rule to any kind of experimental data, for example, data obtained from axial or simple shear soil tests, a collection of nested yield surfaces is used. A plastic modulus is associated with each of the yield surfaces, and

$$H' = h' + \frac{\text{trace } \underset{\sim}{Q}}{\{3\underset{\sim}{Q}:\underset{\sim}{Q}\}^{\frac{1}{2}}} B' \tag{9}$$

where h' is the plastic shear modulus and $(h' + B')$ are the plastic bulk moduli associated with f which are mobilized in consolidation tests upon loading and unloading, respectively. The projections of the yield surfaces onto the deviatoric stress subspace thus define regions of constant plastic shear moduli. For a soil element whose anisotropy initially exhibits rotational symmetry about the y-axis, $\alpha_x = \alpha_z = -\alpha_y/2$ and Eq. 8 simplifies to

$$[(\sigma_y'^s - \sigma_x'^s) - \alpha]^2 + C^2(p'^s - \beta)^2 - k^2 = 0 \tag{10}$$

in which $\alpha = 3\alpha_y/2$. The yield surfaces then plot as ellipses in the axisummetric stress plane $(\sigma_x'^s = \sigma_z'^s)$ as shown in Fig. 1. Points C and E on the outer-most yield surface define the critical state conditions (i.e., $H' = 0$) for axial compression and extension loading conditions, respectively [6]. It is assumed that the slopes of the critical state lines OC and OE remain constant during yielding.

The yield surfaces are allowed to change in size as well as to be translated by the stress point. Their associated plastic moduli are also allowed to vary in and, in general, both k and H' are functions of the plastic strain history. They are conveniently taken as functions of invariant measures of the amount of plastic volumetric strains and/or plastic shear distortions, respectively [7].

Complete specification of the model parameters requires the determination of (i) the initial positions and sizes of the yield surfaces together with their associated plastic moduli; (ii) their size and/or plastic modulus changes as loading proceeds, and finally, (iii) the elastic shear G and bulk B moduli. The soil's anisotropy originally develops during its

deposition and subsequent consolidation which, in most practical cases, occurs under no lateral deformations. In the following, the y-axis is vertical and coincides with the direction of consolidation, and the material's anisotropy initially exhibits rotational symmetry about the vertical y-axis. The model parameters required to characterize the behavior of any given soil can then be derived *entirely* from the results of conventional monotonic axial and cyclic strain-controlled simple shear soil tests [7-9]. As an illustration, Tables 1 and 2 give the parameter-values for the Cook's Bayou sand [7] and the Drammen clay [1]. These parameters were determined by using *solely* the results of axial compression/extension soil tests. Figs. 2 and 3 show the model predictions for both axial compression and consolidation/swelling tests, respectively, performed on the Cook's Bayou sand. Figs. 4 and 5 show the model predictions for both undrained axial and simple shear tests, respectively, performed on the Drammen clay (in Fig. 5 τ_h denotes the *average* horizontal shear stress measured experimentally). Fig. 6 shows the model predictions for cyclic stress- and strain-controlled simple shear and axial tests performed on the Drammen clay. Note that the model predictions agree very well with the experimental test results for all cases.

APPLICATION TO SOLUTION OF BOUNDARY VALUE PROBLEMS

Attention is restricted in the following to "quasi-static" loading conditions. The finite element formulation of the above governing equations (Eqs. 1-6) is performed by using the Galerkin procedure (see e.g. Ref. [14]). The class of constitutive equations assumed leads directly to the definition of tangent stiffness matrix. A simple backward difference scheme is adopted for the numerical time integration [11] in transient analysis. Further, in order to increase its accuracy, a predictor-corrector type algorithm is used at each time step (see Ref. [5] for further details). In the following sections, a number of examples are presented which demonstrate the versatility and accuracy of the proposed formulation in solving boundary value problems of interest in soil mechanics.

1. Two-Dimensional Elastoplastic Consolidation [11]

The finite element mesh and problem description are shown in Fig. 7a. A rigid permeable strip footing of width $2B$ is resting on the surface of a soil layer with drainage occurring at the top surface only. The mechanical properties of the soil to be considered in this example are shown in Figs. 2 and 3. The model parameter values (Table 1) have been normalized by dividing them by σ'^{s}_{vs} = vertical effective consolidation stress. The soil deposit is assumed to be normally consolidated, and $\sigma'^{s}_{vc} = \gamma'^{s} z$ where z is the depth measured from the top surface of the deposit, and $\gamma'^{s} = (1-n^{w})\rho_s$. In the following, $n^{w} = 0.7$, $\rho_s/\rho_w = 2.82$, and $k^{ws} = 2.10^{-6}$. The transient response of the soil deposit under the footing load is dependent upon the rate of loading w, $w = \frac{1}{\mu^s}\frac{dh}{dT}$ where $T = \bar{C}_v t/B^2$; $\bar{C}_v = 2\,\mu^s n^w k^{ws}/\rho_w$; and μ^s is selected to be the initial (at time $t=0$) shear modulus at depth $Z = B/2$, (i.e., $\mu^s = 120.0$). At very slow loading rates (i.e., $w \to 0$) the soil deposit's response is fully drained, whereas when the loading rate becomes large (i.e., $w \to \infty$), the deposit behaves in an undrained (i.e. constant volume) fashion. This is illustrated in Fig. 7b which shows the computed load/

settlement curves for various loading rates. These calculations were performed by neglecting changes in geometry (i.e. small strains/displacement), by including the effects of gravity, and by taking $\Delta t_n = \beta \Delta t_{n-1}$ with β=1.1, so that loading could be achieved in 16 steps only.

2. Wave-Offshore Structure-Soil Interaction [12]

In order to make the present study quite specific, attention herein is concentrated on the behavior of a fully saturated clay foundation for which the repeated loading resulting from wave forces during one individual storm is assumed to occur with no volume change. Furthermore, the foundation material is assumed to consist of a homogeneous deposit of Drammen clay (Figs. 4-6).

Due to the necessity of working within limited computation budgets, the problem geometry is transposed into 2-dimensions by assuming that it is of plane strain. Its 2-dimensional finite representation is shown in Fig. 8a. The structure foundation is represented by a strip footing which consists of a thin layer of elements a thousand times stiffer than the supporting soil. Fig. 8b shows the load system and notation. In addition to the static load W due to the dead weight of the structure, the foundation is also subjected to the cyclic inclined eccentric load F due to the wave forces, and Fig. 8c shows the time histories for its components V, H and M over a complete cycle of loading. For the purpose of illustration, $W/ACu = 3.42$ in the following, where $Cu = 0.584\ \sigma'_{vc}$ denotes the static (unsoftened) undrained simple shear strength of the clay, and A the footing area. The computed load-displacement curves for the first 5 cycles of loading are shown in Fig. 8d, from which the progress of the various deformations can easily be traced: δ and d denote the vertical and horizontal displacements of the center of the foundation, respectively, and θ its tilt.

REFERENCES

[1] Anderson, K.H. (1976), "Behavior of Clay Subjected to Undrained Cyclic Loading," Proceedings, BOSS 76 Conf., Tronheim, Norway, Vol. 1, pp. 392-403.

[2] Biot, M.A. (1955), "Theory of Elasticity and Consolidation for a Porous Anisotropic Solid," J. Applied Physics, Vol. 26, pp. 182-185.

[3] Forrest, J.H., et al. (1976), "Experimental Relationships Between Moduli for Soil Layers Beneath Concrete Pavements," Report No. FAA-RD-76-206.

[4] Hill, R. (1958), "A General Theory of Uniqueness and Stability in Elastic-Plastic Solids," J. Mech. Phys. Solids, Vol. 6, pp. 236-249.

[5] Hughes, T.J.R. and J.H. Prevost (1979), "DIRT II - A Nonlinear Quasi-Static Finite Element Analysis Program," California Institute of Technology, Pasadena, California.

[6] Hvorslev, M.J. (1937), "Uber die Festigkeitseigenschaften gestorler bindiger boden," Ingeniozvidenskabelige Skrifter, A. no. 45, Copenhagen.

[7] Prevost, J.H. (1977), "Mathematical Modeling of Monotonic and Cyclic Undrained Clay Behavior," Int. J. Num. Analyt. Methods in Geomechanics, Vol. 1, No. 2, pp. 195-216.

[8] Prevost, J.H. (1978), "Anisotropic Undrained Stress-Strain Behavior of Clays," J. Geotech. Eng. Div., ASCE, Vol. 104, No. GT8, 1978, pp. 1075-1090.

[9] Prevost, J.H. (1978), "Plasticity Theory for Soil Stress-Strain Behavior," J. Eng. Mech. Div., ASCE, Vol. 104, No. EM5, pp. 1177-1194.

[10] Prevost, J.H. (1980), "Mechanics of Continuous Porous Media," Int. J. of Engineering Science (to appear).

[11] Prevost, J.H. (1980), "Consolidation of Anelastic Porous Media," J. Eng. Mech. Div., ASCE (in process).

[12] Prevost, J.H. Hughes, T.J.R and M.F. Cohen (1980), "Analysis of Gravity Offshore Structure Foundations," Journal of Petroleum Technology (to appear).

[13] Terzaghi, K. (1943), Theoretical Soil Mechanics, Wiley, New York.

[14] Zienkiewicz, O.C. (1977), The Finite Element Method, McGraw Hill.

TABLE 1: COOK'S BAYOU SAND σ'_{vc} = 50 psi - MODEL PARAMETERS

G_1 = 2000 psi, B_1 = 22920 psi, n = 0.5, λ = 148.1

m	$\alpha^{(m)}$ (psi)	$\beta^{(m)}$ (psi)	$k^{(m)}$ (psi)	h_m (psi)	H'_m (psi)	A_m
2	24.00	60.24	32.36	27640.00	-4865.00	-0.1384
3	28.07	60.91	36.39	23870.00	-5724.00	-0.2380
4	32.16	61.39	40.23	20300.00	-5892.00	-0.3446
5	37.28	60.68	43.63	14830.00	-5041.00	-0.6810
6	41.54	61.57	48.25	12870.00	-4588.00	-0.7750
7	46.05	62.47	53.10	10550.00	-3870.00	-0.8636
8	45.68	61.66	64.61	6476.00	-2485.00	-1.020
9	42.95	65.29	77.47	5005.00	-1896.00	-0.9069
10	45.78	68.33	88.34	3599.00	-1475.00	-0.9391
11	44.31	74.75	105.80	2617.00	-1234.00	-0.8995
12	48.00	85.24	127.90	2011.00	-909.90	-0.8694
13	66.66	93.18	153.00	1379.00	-574.20	-1.062
14	87.23	109.50	196.30	619.70	-286.60	-1.068
15	122.60	131.50	261.50	0.00	0.00	-1.113

TABLE 2: DRAMMEN CLAY OCR = 4 - MODEL PARAMETERS

G_1 = 200 σ'_{vc}

m	$\alpha^{(m)}/\sigma'_{vc}$	$k^{(m)}/\sigma'_{vc}$	h_m/σ'_{vc}
2	0.100	0.300	266.667
3	0.150	0.350	133.333
4	0.300	0.600	100.000
5	0.400	0.700	73.333
6	0.475	0.775	54.667
7	0.525	0.875	40.000
8	0.550	0.950	31.000
9	0.575	1.025	24.333
10	0.600	1.050	17.333
11	0.575	1.125	13.333
12	0.550	1.200	10.000
13	0.550	1.250	6.667
14	0.525	1.275	3.333
15	0.467	1.373	0.000

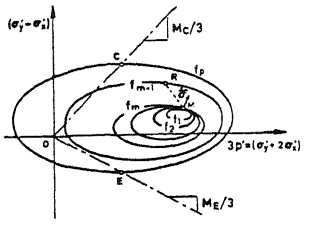

Fig. 1:
Field of Yield Surfaces

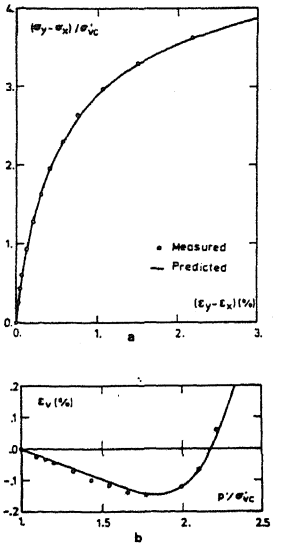

Fig. 2: Cook's Bayou Sand: Axial Compression Tests

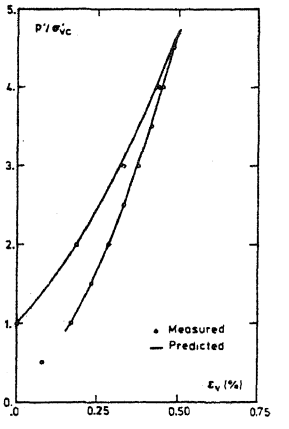

Fig. 3
Cook's Bayou Sand: Consolidation/ Swelling Tests

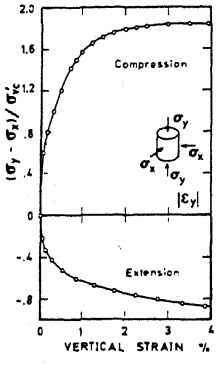

Fig. 4:

Drammen Clay: Axial Tests

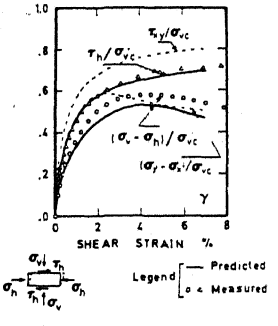

Fig. 5:

Drammen Clay:
Simple Shear Tests

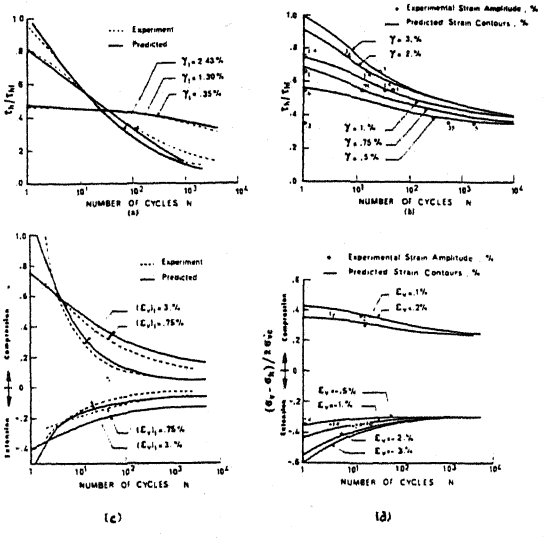

Fig. 6:

Drammen Clay, Cyclic Tests:

Simple Shear	Axial
(a) Strain-controlled	(a) Strain-controlled
(b) Stress-controlled	(b) Stress-controlled

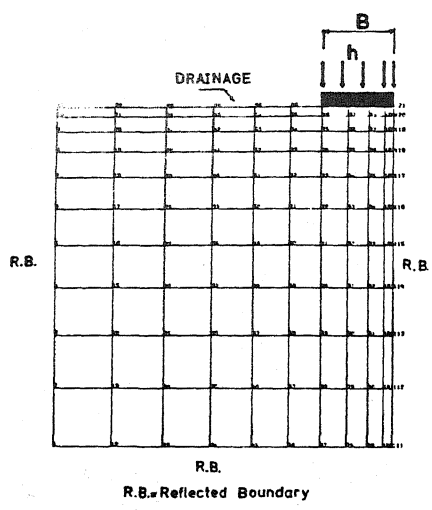

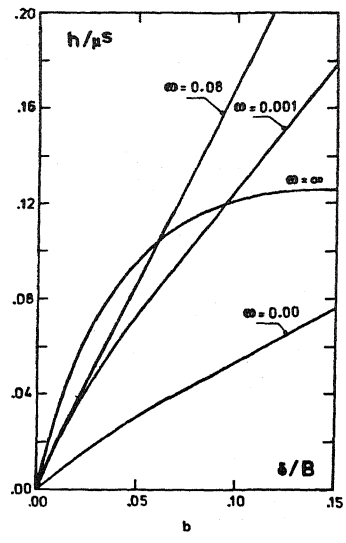

Fig. 7:

Anelastic Consolidation

(a) Finite Element Mesh (b) Load Displacement

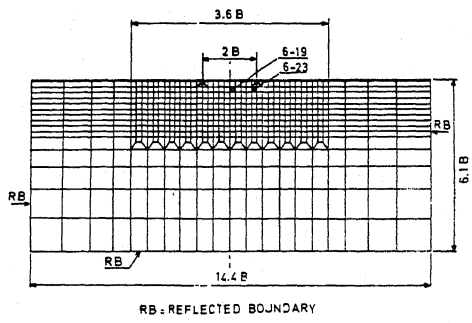

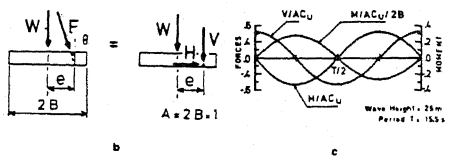

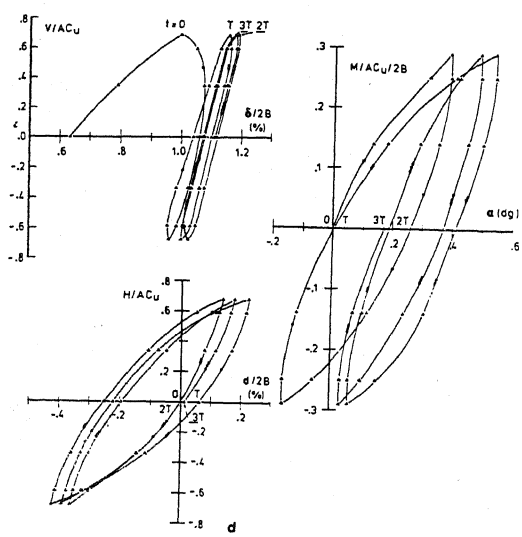

Fig. 8

Wave-Offshore Structure-Soil Interaction:

(a) Finite Element Mesh
(b) Loading Conditions
(c) Wave Load Time Functions
(d) Computed Displacements